Supplementary Information (SI) for Green Chemistry.
This journal is © The Royal Society of Chemistry 2025

Supplementary Information for

Room-Temperature Chromatographic H_2/D_2 Separation via Solid Dihydrogen Complex with Balanced Thermodynamics and Kinetics

Tamon Yamauchi,[1] Taku Kitayama,[1] Kaiji Uchida,[1,2] Nino Keuzenkamp,[1] Hiroaki Iguchi,[3] Ryojun Toyoda,[1] Ryota Sakamoto,[1] Hao Xue,[1] Naoki Kishimoto,[1] Shin-ichiro Noro,[4] Shinya Takaishi[1,5]*

[1]Department of Chemistry, Graduate School of Science, Tohoku University, 6-3 Aramaki-Aza-Aoba, Aoba-Ku, Sendai 980-8578, Japan. Tel: +81-22-795-6545.

[2]Tokyo Metropolitan Industrial Technology Research Institute, 2-4-10 Aomi, Koto, Tokyo 135-0064, Japan

[3]Department of Materials Chemistry, Graduate school of Engineering, Nagoya University, Furo-cho, Chikusa-ku, Nagoya 464-8603, Japan

[4]Faculty of Environmental Earth Science, Hokkaido University, Sapporo 060-0810, Japan

[5]Physical and Chemical Research Infrastructure Group, RIKEN SPring-8 Center, RIKEN, Sayo, Hyogo, 679–5198 Japan

*Correspondence: shinya.takaishi.d8@tohoku.ac.jp

Contents

Experimental Details····· 2
Table S1 Equilibrium constant (*K*) and saturation volumes for H_2 adsorption on **Mn-PCy3**····· 4
Table S2 Equilibrium constant (*K*) and saturation volumes for D_2 adsorption on **Mn-PCy3**····· 4
Table S3 Thermodynamic Parameters of H_2 and D_2 adsorption in **Cu-MFU-4*l***, **Mn-PCy3** and **Mn-dppe**····· 5
Fig. S1 Model structure of (a) **Mn-PCy3-H_2^+** and (b) **Mn-dppe-H_2^+** and (c) **Cu-MFU-4l-H_2** used quantum chemical calculations. ···· 5
Table S4 Computed thermodynamic parameters for H_2 and D_2 adsorption of **Mn-PCy3$^+$** with various functional and basis sets. ····· 6
Table S5 Computed thermodynamic parameters for H_2 and D_2 adsorption of **Cu-MFU-4*l*** with various functional and basis sets. ····· 6
Table S6 Computed thermodynamic parameters for H_2 and D_2 adsorption of **Mn-dppe$^+$** with various functional and basis sets. ····· 7
Fig. S2 Molecular Structures of a series of dihydrogen complexes used for the quantum chemical calculations. ····· 8
Fig. S3-S22 Partial vibrational density of states (p-vDOS) for H_2 and D_2 molecules in compound a to t. ·····9-15
Table S7 Summary of the calculated thermodynamic parameters and H_2/D_2 separation factors. ····· 16
Table S8 Summary of the calculated vibrational frequencies in the compounds. ····· 17
Fig. S23 Correlation between the vibrational frequencies of $\nu_{H\text{-}H}$, $\nu_{M\text{-}H}$(asym) and $\nu_{M\text{-}H}$(asym), and K_{D2}/K_{H2}@298 K····· 18
Fig. S24 in-situ PXRD patterns of (a) Mn-PCy3 and (b) Mn-dppe (under vacuum and under 1 bar H_2). ····· 19
Estimation of Energy Cost of PSA process·····20-21
References····· 22

Experimental Details

I. Adsorption measurement

H_2 and D_2 sorption isotherm was performed using microtracbel Belsorp Max. H_2 sorption isotherm was measured by using G1 grade (> 99.99999 %) H_2 gas. Sorption measurement was performed by volumetric method, and the volume of adsorbed H_2 gas was calculated from the ideal gas equation with second virial coefficient of 3.436×10^{-9}. H_2 sorption isotherm was measured for $[Mn(CO)_3(PCy_3)_2][BARF]$ at the temperature of 213, 223, 233, 243, 253, 263, and 273 K. Temperature control during sorption measurement was done by using Technosigma UCR-150N-S cryostat. Adsorption isotherm was measured in the pressure range of P = 0.001 - 0.98 bar and desorption isotherm was measured down to P/P_0 = 0.01. The volume of sample space was measured after sorption measurement by using G2 grade (> 99.999 %) He gas, and dead volume correction was applied to the raw data.

II. DFT calculation

DFT calculation was performed to investigate the thermodynamic properties of hydrogen adsorption with using GAUSSIAN 16 software.[S1] Geometry optimization and frequency analysis were performed using wB97X-D functional and def2-TZVP, cc-pVDZ, and 6-31G basis sets for Mn, H_2 or D_2, and others, respectively. Thermodynamic parameters were obtained by following procedure. For the calculation of thermodynamic parameters, the counterpoise correction by considering basis set superposition error (BSSE)[S2] for **comp-H_2** was applied.[S3]

Geometry optimization and vibrational analysis were performed for the singlet spin state of coordinatively-unsaturated (16-electron) complexes $[Mn(PCy_3)_2(CO)_3](BARF)$, H_2- or D_2-adduct of each complexes $[Mn(\eta^2\text{-}H_2$ or $\text{-}D_2)(PCy_3)_2(CO)_3](BARF)$ and free H_2 or D_2 molecule. For 16-electron complexes, initial structure was derived from the crystal structure data[S4] For H_2-adduct, initial structures were made by adding a H_2 molecule to the optimized structure of the 16-electron complexes.

Standard molar Gibbs free energy change $\Delta G°_{ads}$, standard molar enthalpy change $\Delta H°_{ads}$ and standard molar entropy change $\Delta S°_{ads}$ of adsorption were calculated by following equation

$$\Delta H°_{ads} = H° (\mathbf{1^+\text{-}H_2}) - H° (\mathbf{1^+}) - H° (\mathbf{H_2})$$

$$\Delta G°_{ads} = G° (\mathbf{1^+\text{-}H_2}) - G° (\mathbf{1^+}) - G° (\mathbf{H_2})$$

$$\Delta S°_{ads} = (\Delta H°_{ads} - \Delta G°_{ads}) / 298.15$$

where the subscript M-H_2, H_2 and M represent H_2-adduct, free H_2 molecule and 16-electron complex, respectively.

III. Syntheses

Materials. $Mn(CO)_5Br$ was purchased from Aldrich. Tricyclohexylphosphine (PCy_3) was purchased from Fujifilm Wako pure chemical corporation, and used without further purification.

Synthesis of *mer-trans*-[$MnBr(CO)_3(PCy_3)_2$]

This procedure was a modification of one in the literature.[S4] $MnBr(CO)_5$ (0.68 g, 2.47 mmol) and PCy_3 (1.40 g, 5.00 mmol) were placed into 100 mL round-bottom flask, and about 50 mL of toluene was added. The orange solution was irradiated for 24 h with a LED light (Asahi spectra, model CL-H1-365-9-1-B (365 nm)), forming a yellow precipitate. The solid was collected by the suction filtration and washed with hexane. Yield, 1.01 g (1.29 mmol, 52%).

Synthesis of Na[BARF]

This procedure was a modification of one in the literature.[S4] 3,5-Bis(trifluoromethyl)bromobenzene (5.0 mL, 29 mmol) was slowly added to a suspension of anhydrous $NaBF_4$ (0.800 g, 7.29 mmol) and magnesium powder (5.0 g) in 150 mL of diethyl ether. The suspension was stirred for 24 h, producing a brown solution with white precipitate. The solution was exposed to air and quenched with 20 mL of saturated aqueous sodium carbonate solution. The ether layer was collected, and the aqueous layer was washed with fresh ether. The ether layers were combined, dried over magnesium sulfate, and filtered. The solvent was removed in vacuo, and the resulting residue was dissolved in toluene and evaporated. The residue was washed with CH_2Cl_2 and filtered to produce the product as a white powder. Yield, 3.32 g (51.5%).

Synthesis of *mer-trans*-[$Mn(CO)_3(PCy_3)_2$](BARF) (Mn-PCy_3)

This procedure was a modification of one in the literature.[S4] In the argon filled grove box, Na[BARF] (0.44 g, 0.50 mmol) was mixed with *mer*-[$MnBr(CO)_3(PCy_3)_2$] (0.39 g, 0.50 mmol) in a vial, and 10 mL of pre-cooled CH_2Cl_2 (in the freezer) was added to the solid mixture, immediately forming an blackish-green solution that was stirred for 5 min. The precipitate was removed by the filtration with celite. The filtrate was collected, and the solvent was removed in vacuo. The residue was filtered and washed with hexane to produce the product as a dark-green powder. Yield, 0.68 g (87%).

Table S1. Equilibrium constant (K) and saturation volumes for H_2 adsorption on **Mn-PCy3**.

T / K	K / bar^{-1}	V_m / cm^3 g^{-1}
213	3.102	10.56
223	1.648	
233	0.8549	
243	0.4671	
253	0.2727	
263	0.1687	
273	0.1168	

Table S2. Equilibrium constant (K) and saturation volumes for D_2 adsorption on **Mn-PCy3**.

T / K	K / bar^{-1}	V_m / cm^3 g^{-1}
213	12.91	10.56
223	6.033	
233	2.891	
243	1.466	
253	0.7530	
263	0.4136	
273	0.2557	

Table S3 Thermodynamic Parameters of H_2 and D_2 adsorption in **Cu-MFU-4*l***, **Mn-PCy3** and **Mn-dppe**

	[a]**Cu-MFU-4*l***		**Mn-PCy3**		[b]**Mn-dppe**	
	$\Delta H°$ (kJ /mol)	$\Delta S°$ (J / K·mol)	$\Delta H°$ (kJ /mol)	$\Delta S°$ (J / K·mol)	$\Delta H°$ (kJ /mol)	$\Delta S°$ (J / K·mol)
H_2	–32.6 ± 0.2	–105.6 ± 0.9	–27.0 ± 0.4	–117.0 ± 1.5	–50.2 ± 0.6	–121.7 ± 1.8
D_2	–35.0 ± 0.1	–111.7± 0.9	–32.0 ± 0.3	–128.7 ± 1.1	–54.4 ± 0.4	–129.3 ± 1.3

[a]Cited from ref. 14. [b]Cited from ref. 28.

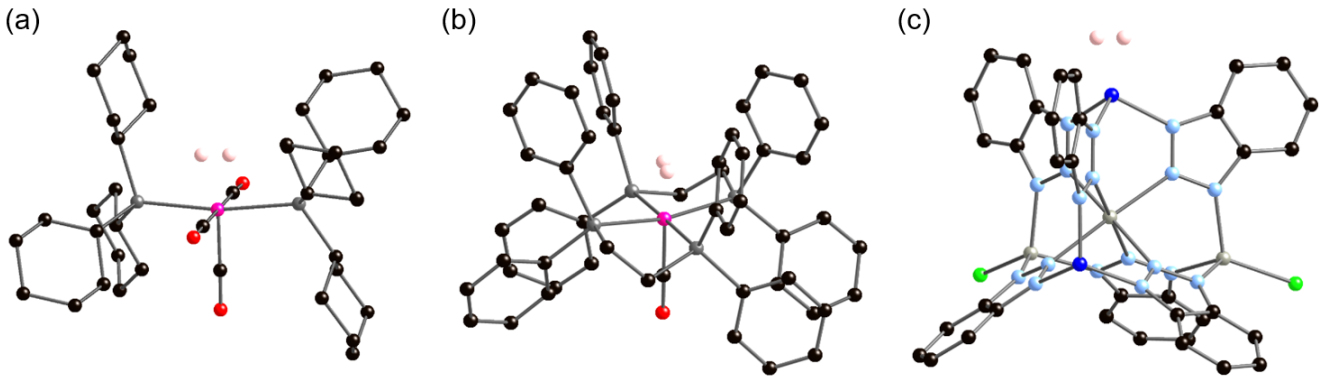

Fig. S1 Model structure of (a) **Mn-PCy3-H_2^+** and (b) **Mn-dppe-H_2^+** and (c) **Cu-MFU-4l-H_2** used quantum chemical calculations. Deep pink: Mn, Deep blue: Cu, Silver: Zn, Gray: P, Black: C, Red: O, Light blue: N, Light Green: Cu, Light pink: H. Hydrogen atoms in the ligand are omitted for clarity.

Table S4 Computed thermodynamic parameters for H_2 and D_2 adsorption of **Mn-PCy3**$^+$ with various functional and basis sets.

entry	Functional	Basis sets			ΔH°(H_2) kJ /mol	ΔH°(D_2) kJ /mol	ΔΔH° kJ /mol	α @298K
		Mn	H_2 (D_2)	others				
1	B3LYP	def2-TZVP	cc-pVDZ	6-31G	–25.18	–29.45	4.27	2.42
2	B3LYP	def2-TZVP	aug-cc-pVDZ	6-31G	–25.29	–29.54	4.25	2.40
3	M06	def2-TZVP	cc-pVDZ	6-31G	–31.01	–35.73	4.72	2.69
4	M06	def2-TZVP	aug-cc-pVDZ	6-31G	–31.80	–36.47	4.67	2.65
5	wB97X-D	def2-TZVP	cc-pVDZ	6-31G	–28.02	–32.54	4.51	2.57
6	wB97X-D	def2-TZVP	aug-cc-pVDZ	6-31G	–28.47	–32.99	4.52	2.59

Table S5 Computed thermodynamic parameters for H_2 and D_2 adsorption of **Cu-MFU-4l** with various functional and basis sets.

entry	Functional	Basis sets			ΔH°(H_2) kJ / mol	ΔH°(D_2) kJ / mol	ΔΔH° kJ / mol	α @298K
		H2-bindingCu	H_2 (D_2)	others				
1	B3LYP	def2-TZVP	cc-pVDZ	6-31G	–26.71	–28.58	1.87	1.00
2	B3LYP	def2-TZVP	aug-cc-pVDZ	6-31G	–27.13	–29.02	1.89	0.97
3	M06	def2-TZVP	cc-pVDZ	6-31G	–33.92	–36.05	2.11	1.33
4	M06	def2-TZVP	aug-cc-pVDZ	6-31G	–35.12	–37.25	2.13	1.32
5	wB97X-D	def2-TZVP	cc-pVDZ	6-31G	–36.07	–38.21	2.14	1.38
6	wB97X-D	def2-TZVP	aug-cc-pVDZ	6-31G	–36.80	–38.98	2.18	1.39

Table S6 Computed thermodynamic parameters for H_2 and D_2 adsorption of **Mn-dppe**$^+$ with various functional and basis sets.

entry	Functional	Basis sets			ΔH°(H_2) kJ / mol	ΔH°(D_2) kJ / mol	ΔΔH° kJ / mol	α @298K
		H2-bindingCu	H_2 (D_2)	others				
1	B3LYP	def2-TZVP	cc-pVDZ	6-31G	–33.12	–37.35	4.22	3.09
2	B3LYP	def2-TZVP	aug-cc-pVDZ	6-31G	–33.06	–37.13	4.07	2.27
3	M06	def2-TZVP	cc-pVDZ	6-31G	–50.76	–55.19	4.43	2.56
4	M06	def2-TZVP	aug-cc-pVDZ	6-31G	–51.39	–55.75	4.36	2.43
5	wB97X-D	def2-TZVP	cc-pVDZ	6-31G	–48.01	–52.57	4.56	2.54
6	wB97X-D	def2-TZVP	aug-cc-pVDZ	6-31G	–48.29	–52.86	4.56	2.56

Table S7 Computed separation factors between each hydrogen molecule isotope pair.

	H_2	HD	HT	D_2	DT	T_2
H_2	1	1.57	1.87	2.59	2.95	3.52
HD		1	1.19	1.65	1.89	2.25
HT			1	1.38	1.58	1.88
D_2				1	1.14	1.36
DT					1	1.19
T_2						1

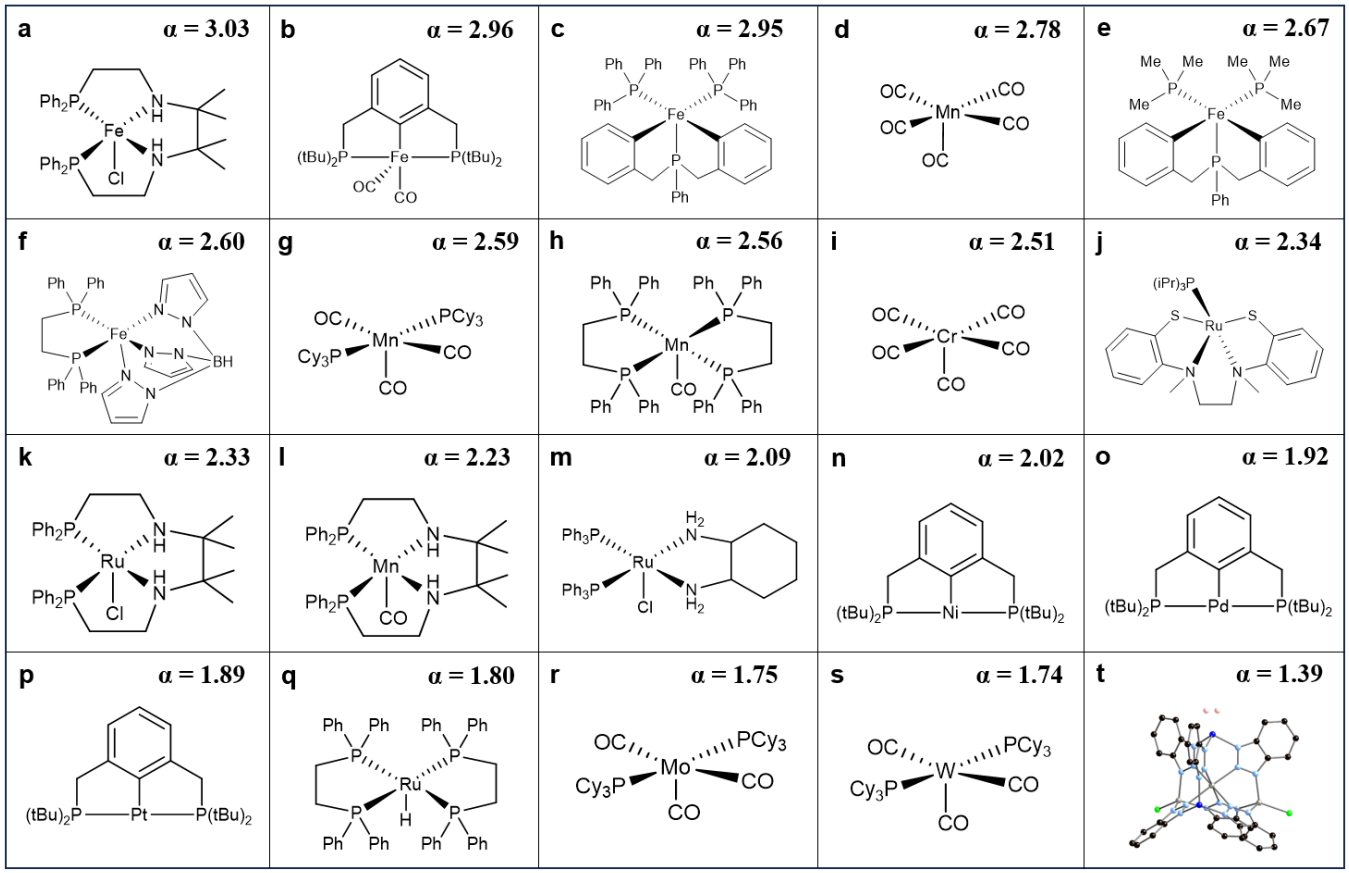

Fig. S2 Molecular Structures of a series of dihydrogen complexes used for the quantum chemical calculations. α values represent the calculated H_2/D_2 separation factors at 298 K.

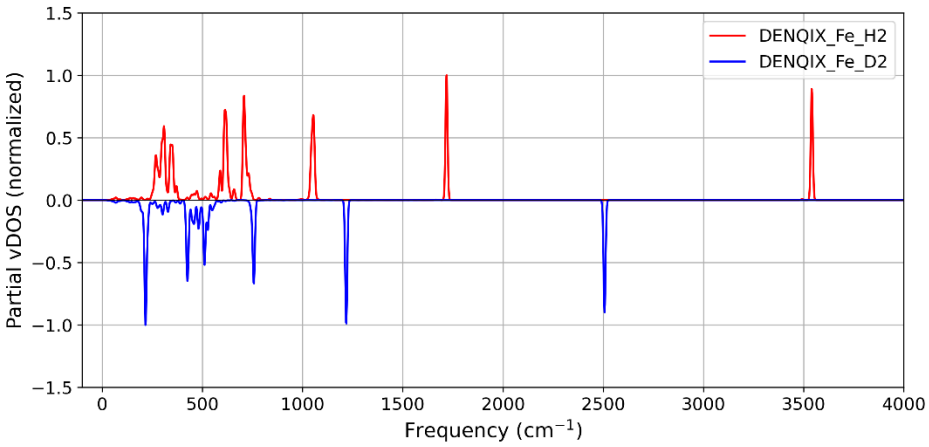

Fig. S3 Partial vibrational density of states (p-vDOS) for H_2 and D_2 molecules in compound **a**.

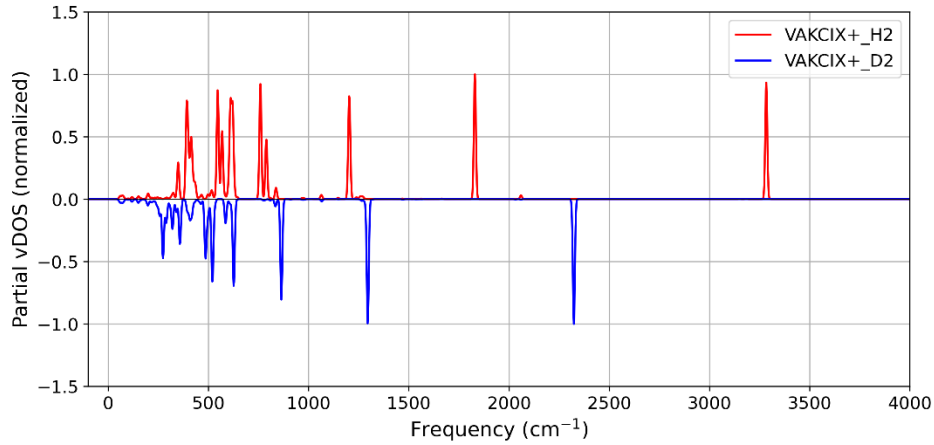

Fig. S4 Partial vibrational density of states (p-vDOS) for H_2 and D_2 molecules in compound **b**.

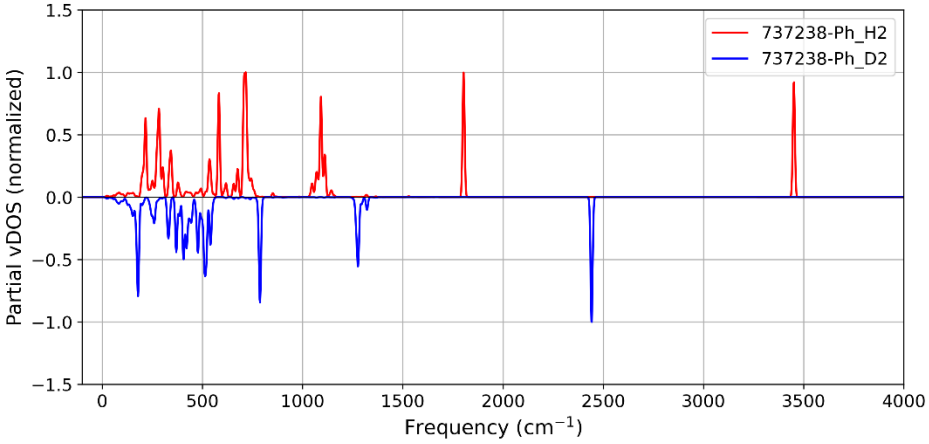

Fig. S5 Partial vibrational density of states (p-vDOS) for H_2 and D_2 molecules in compound **c**.

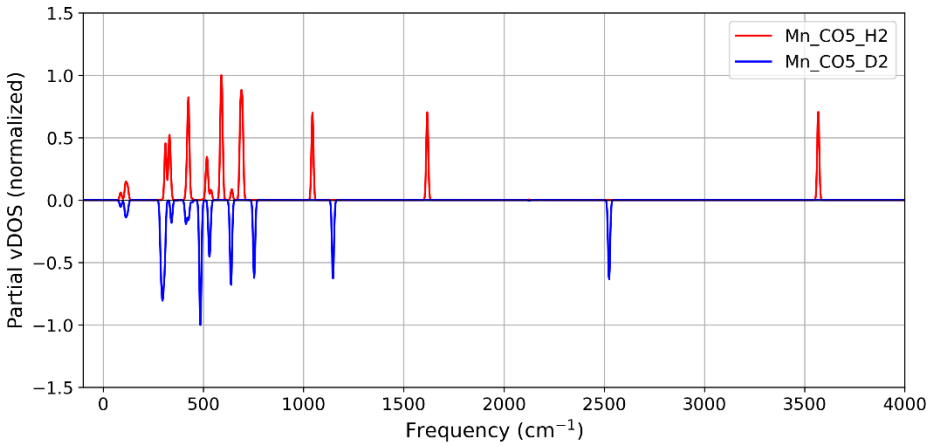

Fig. S6 Partial vibrational density of states (p-vDOS) for H_2 and D_2 molecules in compound **d**.

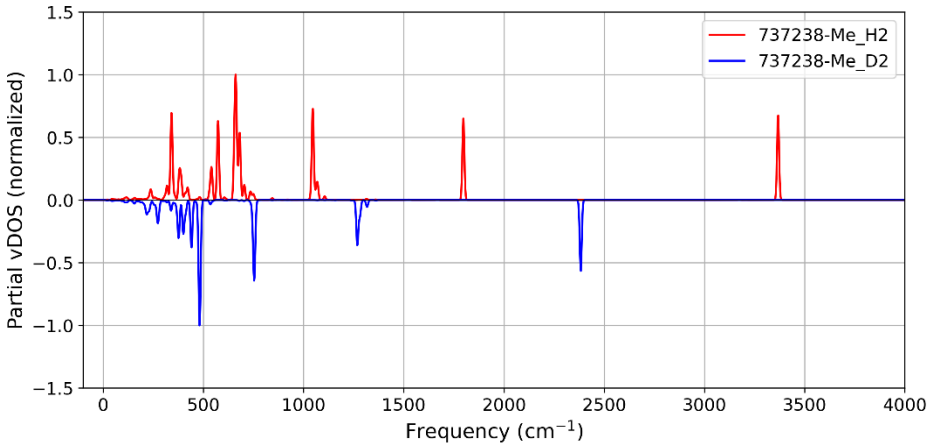

Fig. S7 Partial vibrational density of states (p-vDOS) for H_2 and D_2 molecules in compound **e**.

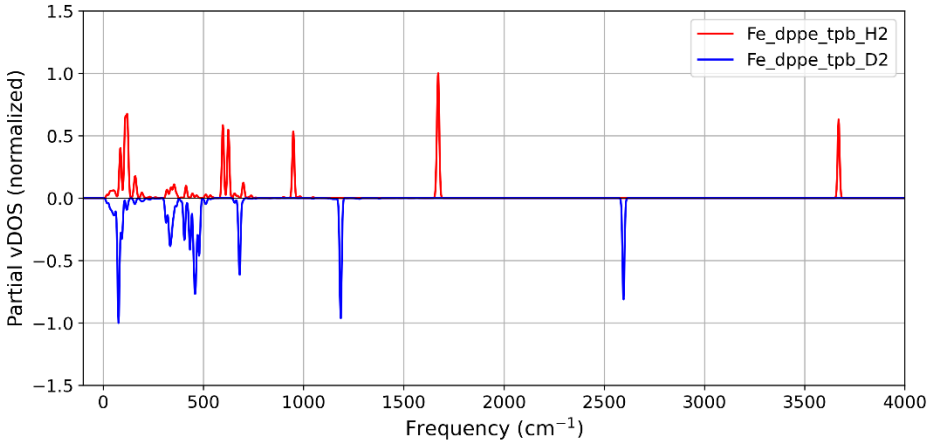

Fig. S8 Partial vibrational density of states (p-vDOS) for H_2 and D_2 molecules in compound **f**.

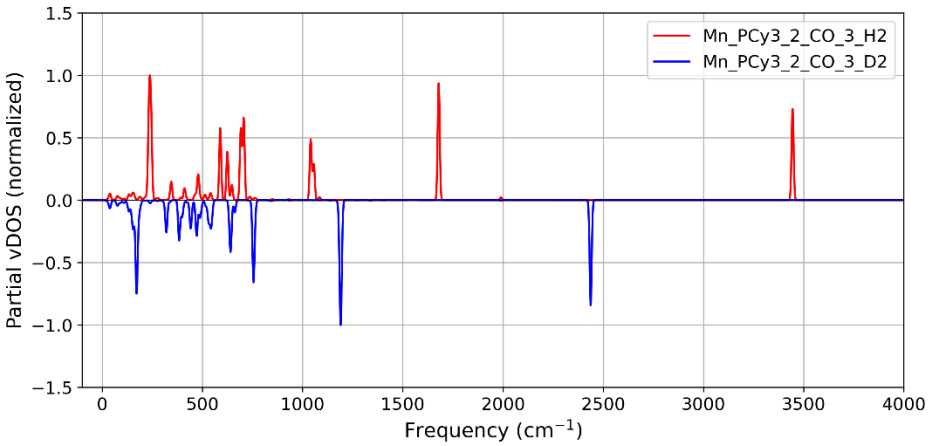

Fig. S9 Partial vibrational density of states (p-vDOS) for H_2 and D_2 molecules in compound **g**.

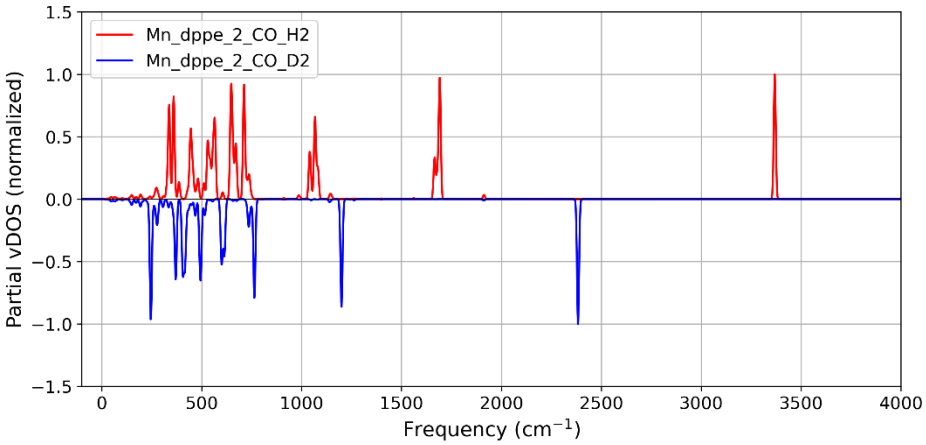

Fig. S10 Partial vibrational density of states (p-vDOS) for H_2 and D_2 molecules in compound **h**.

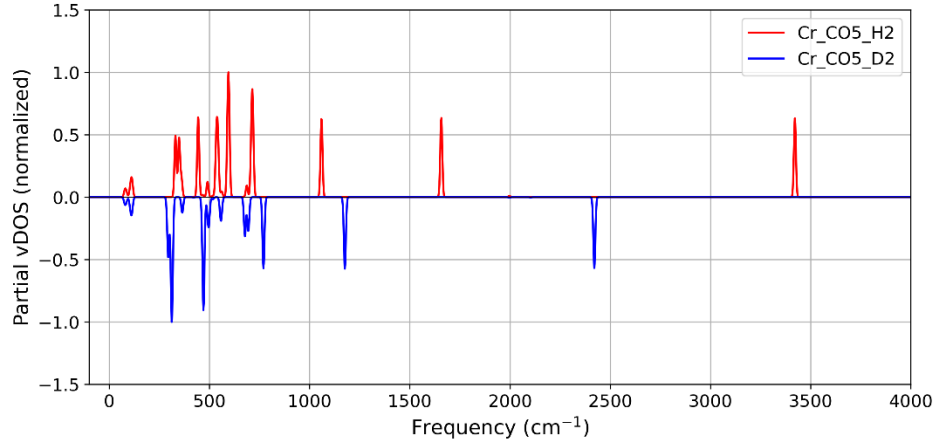

Fig. S11 Partial vibrational density of states (p-vDOS) for H_2 and D_2 molecules in compound **i**.

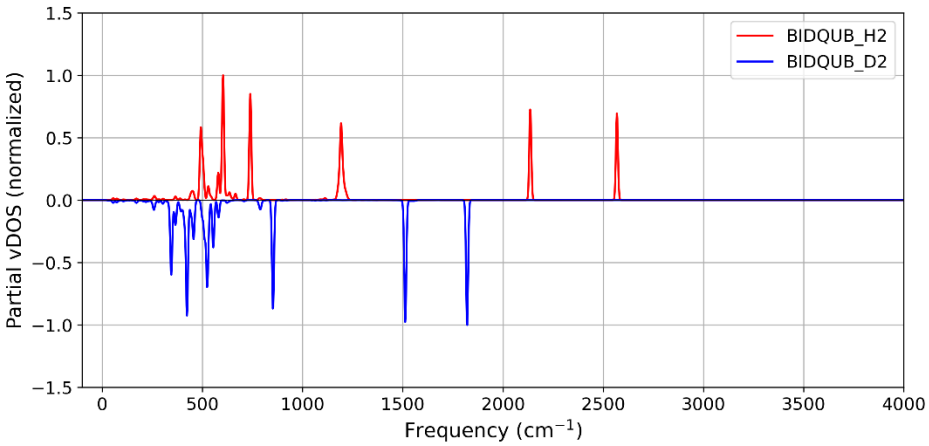

Fig. S12 Partial vibrational density of states (p-vDOS) for H_2 and D_2 molecules in compound **j**.

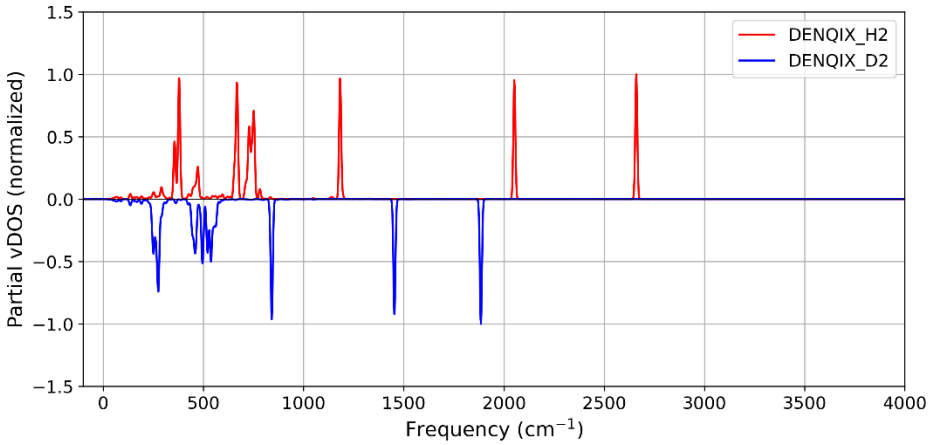

Fig. S13 Partial vibrational density of states (p-vDOS) for H_2 and D_2 molecules in compound **k**.

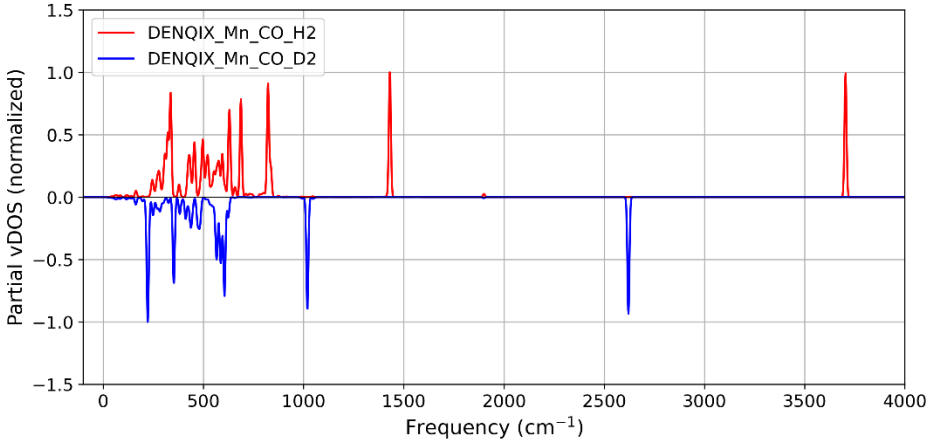

Fig. S14 Partial vibrational density of states (p-vDOS) for H_2 and D_2 molecules in compound **l**.

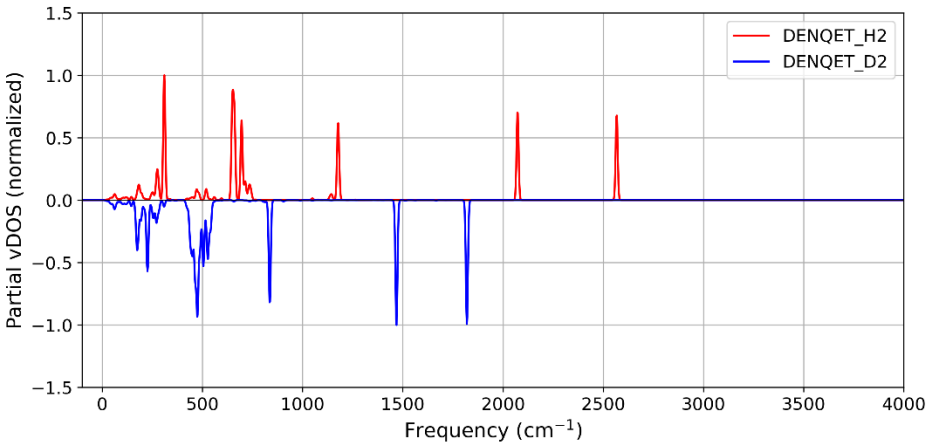

Fig. S15 Partial vibrational density of states (p-vDOS) for H_2 and D_2 molecules in compound **m**.

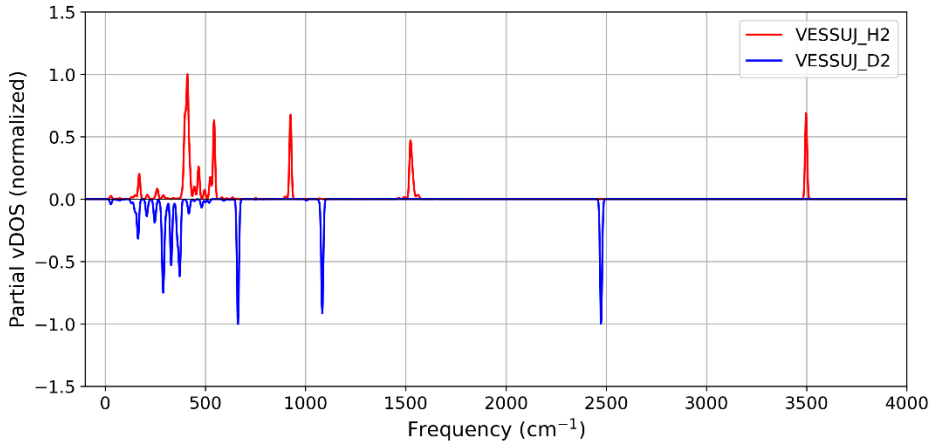

Fig. S16 Partial vibrational density of states (p-vDOS) for H_2 and D_2 molecules in compound **n**.

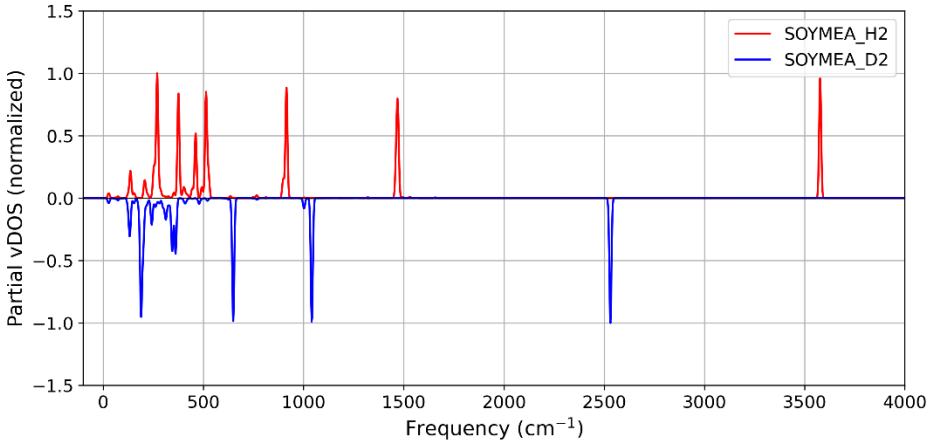

Fig. S17 Partial vibrational density of states (p-vDOS) for H_2 and D_2 molecules in compound **o**.

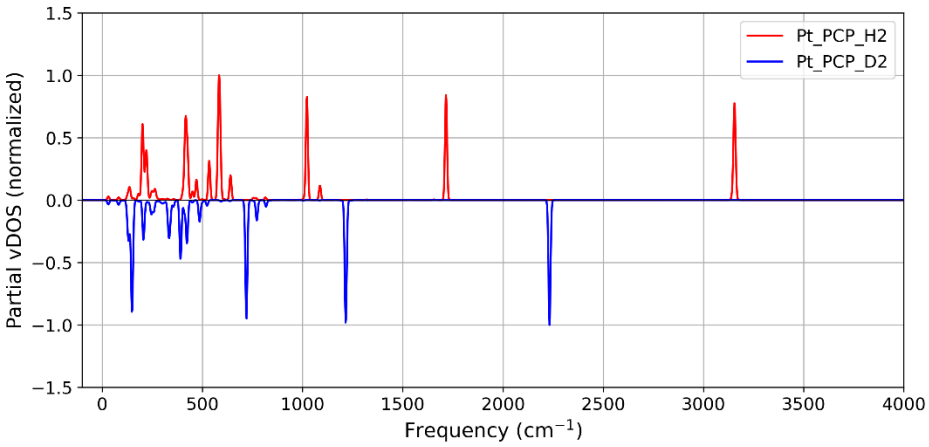

Fig. S18 Partial vibrational density of states (p-vDOS) for H_2 and D_2 molecules in compound **p**.

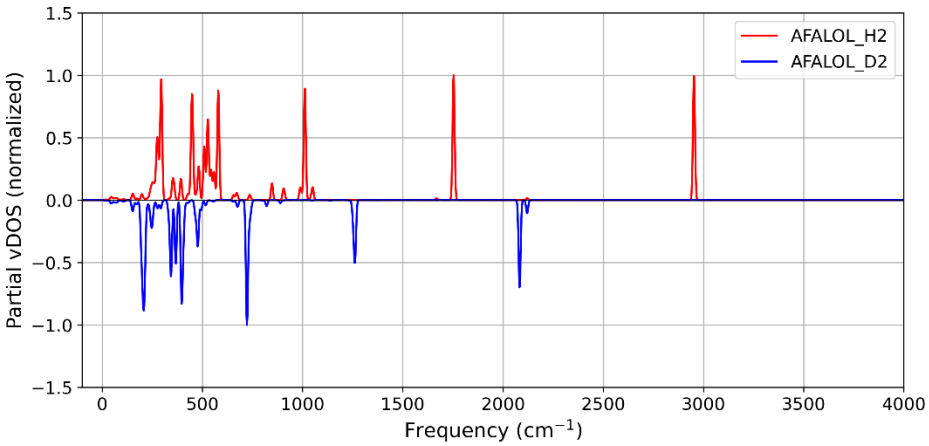

Fig. S19 Partial vibrational density of states (p-vDOS) for H_2 and D_2 molecules in compound **q**.

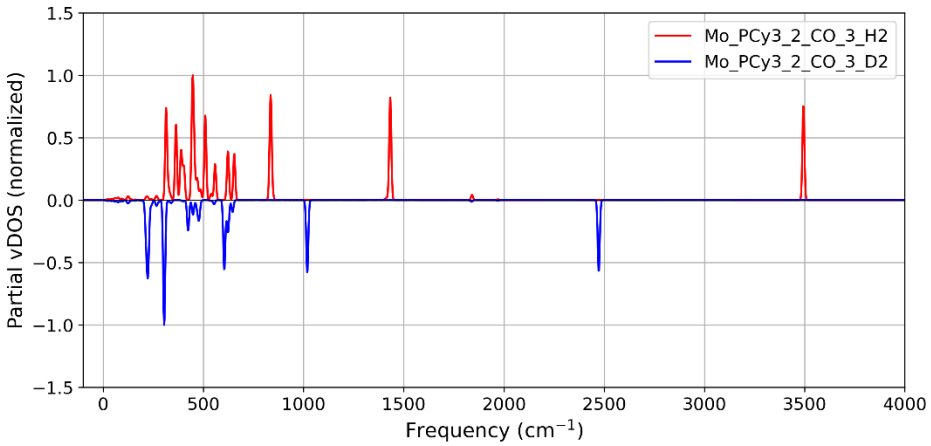

Fig. S20 Partial vibrational density of states (p-vDOS) for H_2 and D_2 molecules in compound **r**.

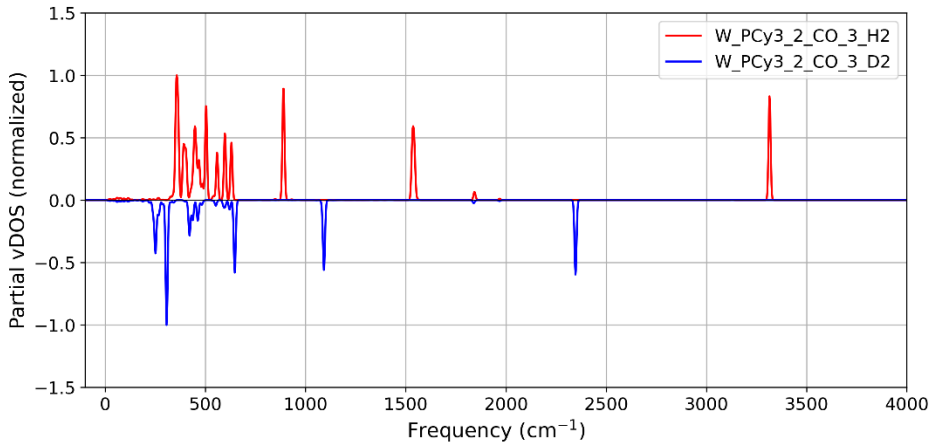

Fig. S21 Partial vibrational density of states (p-vDOS) for H_2 and D_2 molecules in compound **s**.

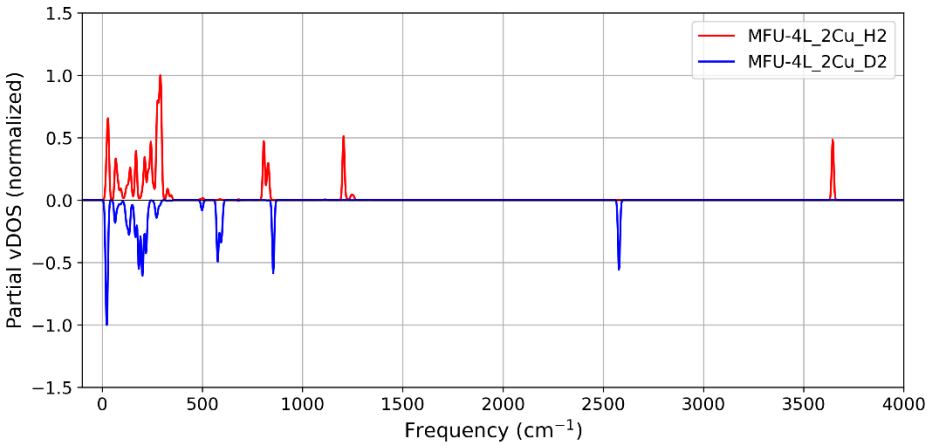

Fig. S22 Partial vibrational density of states (p-vDOS) for H_2 and D_2 molecules in compound **t**.

Table S8 Summary of the calculated thermodynamic parameters and H_2/D_2 separation factors.

Symbol	$\Delta H°(H_2)$ (kJ/mol)	$\Delta G°(H_2)$ (kJ/mol)	$\Delta H°(D_2)$ (kJ/mol)	$\Delta G°(D_2)$ (kJ/mol)	$\Delta\Delta H°$ (kJ/mol)	$\Delta\Delta G°$ (kJ/mol)	α at 298K	H-H distance (Å)
a	-39.70	2.52	-44.65	-0.23	4.95	2.75	3.03	0.804
b	-33.91	5.65	-38.94	2.96	5.03	2.69	2.96	0.824
c	-34.17	8.70	-39.08	6.02	4.91	2.68	2.95	0.811
d	-50.87	-12.95	-55.62	-15.48	4.75	2.53	2.78	0.803
e	-10.16	29.61	-14.8	27.18	4.64	2.43	2.67	0.817
f	2.61	37.00	-1.87	34.63	4.48	2.37	2.60	0.795
g	-26.17	-0.74	-30.69	-3.10	4.52	2.36	2.59	0.811
h	-48.32	-11.63	-52.89	-13.96	4.57	2.33	2.56	0.815
i	-41.10	-3.90	-45.54	-6.18	4.44	2.28	2.51	0.811
j	-83.63	-43.74	-88.21	-45.85	4.58	2.11	2.43	0.916
k	-105.01	-61.30	-109.58	-63.40	4.57	2.10	2.33	0.899
l	-23.66	15.95	-27.63	13.96	3.97	1.99	2.23	0.790
m	-103.99	-59.50	-108.16	-61.33	4.17	1.83	2.09	0.914
n	-66.85	-28.11	-70.52	-29.85	3.67	1.74	2.02	0.808
o	-59.32	-23.04	-62.70	-24.65	3.38	1.61	1.92	0.803
p	-80.47	-41.96	-83.99	-43.54	3.52	1.58	1.89	0.842
q	-77.21	-37.18	-80.74	-38.63	3.53	1.45	1.80	0.855
r	-56.24	-13.73	-59.4	-15.11	3.16	1.38	1.75	0.803
s	-61.69	-19.96	-64.93	-21.33	3.24	1.37	1.74	0.816
t	-36.80	-8.38	-38.98	-9.19	2.18	0.81	1.39	0.798

Table S9 Summary of the calculated vibrational frequencies (cm^{-1}) in the compounds.

symbol	H-H Stretch (H_2)	M-H Asym (H_2)	M-H Sym (H_2)	H-H Stretch (D_2)	M-H Asym (D_2)	M-H Sym (D_2)
a	3541.11	1718.35	1055.22	2507.00	1217.79	758.38
b	3284.02	1829.90	1204.25	2323.86	1295.41	864.23
c	3451.49	1803.55	1091.52	2442.33	1277.54	787.82
d	3568.29	1617.27	1044.13	2524.64	1146.66	753.33
e	3367.88	1797.39	1045.70	2383.15	1267.84	753.77
f	3670.04	1672.90	950.23	2596.36	1185.13	680.54
g	3445.23	1679.30	1040.47	2437.66	1193.10	754.52
h	3368.60	1691.78	1066.68	2383.94	1199.80	763.91
i	3421.85	1657.18	1059.6	2421.04	1176.10	769.90
j	2568.71	2136.38	1189.34	1821.11	1512.68	852.45
k	2660.15	2051.76	1182.50	1884.85	1453.31	841.34
l	3704.3	1430.57	822.48	2621.06	1018.96	569.45
m	2567.48	2072.97	1181.67	1820.03	1468.61	836.23
n	3497.73	1522.41	924.59	2474.68	1083.55	662.53
o	3577.79	1464.13	914.58	2531.09	1041.02	648.95
p	3153.37	1715.75	1021.34	2232.35	1215.39	719.76
q	2953.13	1753.61	1011.18	2083.10	1261.85	721.85
r	3494.36	1430.77	836.88	2472.99	1018.50	604.38
s	3315.49	1532.69	889.06	2347.16	1091.77	646.52
t	3645.55	1204.31	806.41	2579.08	853.60	597.01

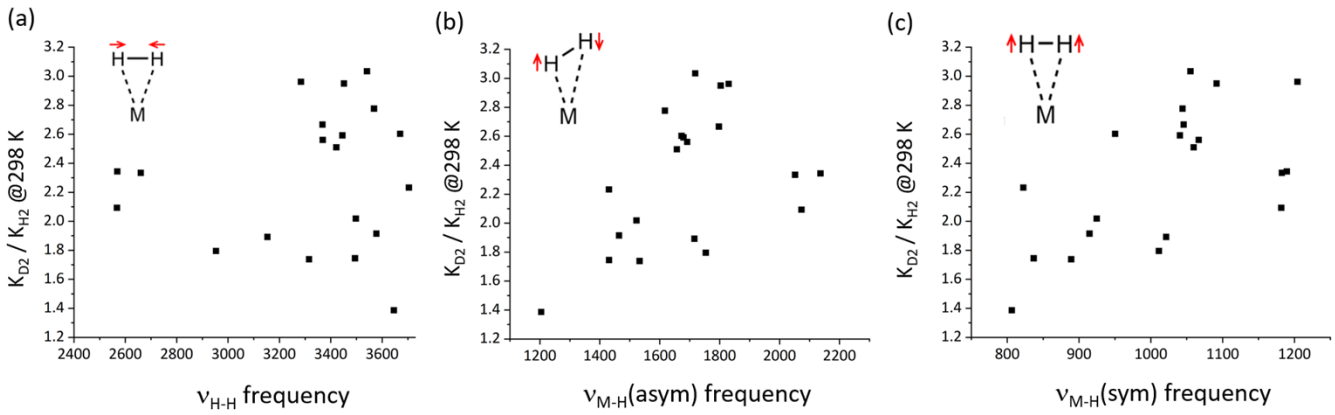

Fig. S23 Correlation between the vibrational frequencies of (a) ν_{H-H}, (b) ν_{M-H}(asym) and ν_{M-H}(asym), and K_{D2}/K_{H2}@298 K in the compounds shown in Fig. S2, respectively.

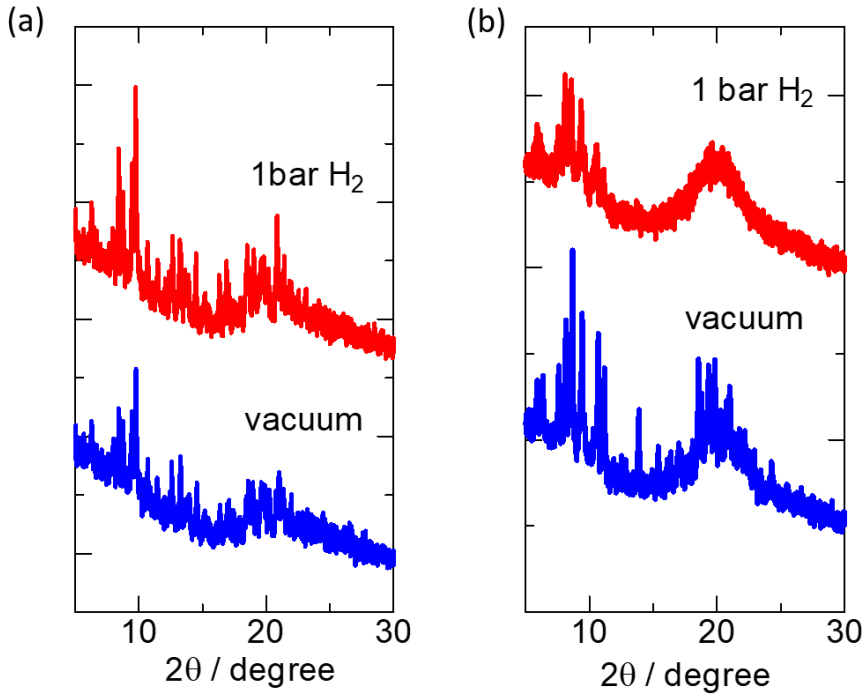

Fig. S24 in-situ PXRD patterns of (a) Mn-PCy3 and (b) Mn-dppe (under vacuum and under 1 bar H_2).

Estimation of Energy Cost of PSA process

We consider enriching an H_2:D_2 = 99:1 mixture to H_2:D_2 = 1:99, yielding 1 mol of product.

Case1: Energy cost for the distillation

The present energy cost for the H_2 liquification is 12.5-15 kWh/kg, corresponding to 90-108 kJ/mol.[S5]

Then, energy for liquefying 100 mol H_2:D_2 = 99:1 to form 1 mol H_2:D_2 = 1:99 is approximately 10,000 kJ.

Case2: Energy cost for the PSA using dihydrogen complex

We assume the following conditions.

α = 3.0, T = 273 K, adsorption at 10 bar, desorption at 1 bar.

In addition, we assume the following competitive adsorption,

$$\frac{\theta_{D2}}{\theta_{H2}} = \alpha\frac{p_{D2}}{p_{H2}}$$

, where θ is adsorbed amount of each gas, p is the partial pressure of each gas.

Number of stages and compressed moles

For a given separation factor, the number of stages needed is

$$n = \lceil log_{\alpha}(\frac{99}{1/99}) \rceil,$$

and the enriched composition in each stage is

$$x_k = \frac{(1/99)\alpha^k}{1 + (1/99)\alpha^k}.$$

The corresponding flow to the next stage is $M_k = 1/x_k$(since we retain ~1 mol of D_2 in each stage). The amount of gas that must be compressed in each stage is the flow from the previous stage.

For $\alpha = 3$, the process requires 9 stages. The compressed amounts in successive stages are:

Stage 1: 100.000 mol → Stage 2: 34.000 → Stage 3: 12.000 → Stage 4: 4.6667 → Stage 5: 2.2222 → Stage 6: 1.4074 → Stage 7: 1.1358 → Stage 8: 1.0453 → Stage 9 (product): 1.0050 mol (D_2 ≈ 99.50%).

Total moles compressed over the first 8 passes (plus the initial 100 mol):

$$N_{\text{comp}} = 100 + \sum_{k=1}^{8} M_k \approx 157.49\ mol.$$

Isothermal compression work (10 → 1 bar at 273 K)

The work to compress 1 mol of ideal gas from 1 bar to 10 bar at temperature $T$is

$w = RTln(\frac{10}{1})$.

At $T = 273$ K:
$w = 8.314 \times 273 \times ln10 \approx 5.23\ kJ/mol.$

3) Total energy and per-product-mol cost

$W_{\text{tot}} = N_{\text{comp}}\, w \approx 157.49 \times 5.226 \approx 823\ kJ.$

Note: In the above estimate, we do not account for compressor efficiency or for energy recovery during isothermal expansion.

References

S1 Gaussian 16, Revision C.01, M. J. Frisch et al., Gaussian, Inc., Wallingford CT (2016).

S2 S. S. Xantheas, *J. Chem. Phys.* **1996**, *104*, 8821–8824.

S3 S. Simon, M. Duran, J. J. Dannenberg, *J. Chem. Phys.*, 1996, **105**, 11024–11031.

S4 A. Toupadakis, G. J. Kubas, W. A. King, B. L. Scott, J. Huhmann-Vincent, *Organometallics*, 1998, **17**, 5315–5323.

S5 S. ZS. Al Ghafri *et al.*, *Energy Environ. Sci.*, 2022,**15**, 2690-2731.